Neurosci. Bull. September, 2020, 36(9):1035–1045
https://doi.org/10.1007/s12264-020-00544-0

www.neurosci.cn
www.springer.com/12264

ORIGINAL ARTICLE

Macrophage–NLRP3 Inflammasome Activation Exacerbates Cardiac Dysfunction after Ischemic Stroke in a Mouse Model of Diabetes

Hong-Bin Lin[1,2,3] · Guan-Shan Wei[1] · Feng-Xian Li[1] · Wen-Jing Guo[1] · Pu Hong[1] · Ya-Qian Weng[1] · Qian-Qian Zhang[1] · Shi-Yuan Xu[1] · Wen-Bin Liang[4] · Zhi-Jian You[2] · Hong-Fei Zhang[1]

Received: 6 October 2019 / Accepted: 17 March 2020 / Published online: 18 July 2020

Abstract Ischemic stroke is one of the leading causes of death worldwide. In the post-stroke stage, cardiac dysfunction is common and is known as the brain–heart interaction. Diabetes mellitus worsens the post-stroke outcome. Stroke-induced systemic inflammation is the major causative factor for the sequential complications, but the mechanism underlying the brain–heart interaction in diabetes has not been clarified. The NLRP3 (NLR pyrin domain-containing 3) inflammasome, an important component of the inflammation after stroke, is mainly activated in M1-polarized macrophages. In this study, we found that the cardiac dysfunction induced by ischemic stroke is more severe in a mouse model of type 2 diabetes. Meanwhile, M1-polarized macrophage infiltration and NLRP3 inflammasome activation increased in the cardiac ventricle after diabetic stroke. Importantly, the NLRP3 inflammasome inhibitor CY-09 restored cardiac function, indicating that the M1-polarized macrophage–NLRP3 inflammasome activation is a pathway underlying the brain–heart interaction after diabetic stroke.

Keywords Ischemic stroke · Diabetes mellitus · Cardiac dysfunction · NLRP3 inflammasome · Macrophage

Introduction

Stroke is the leading cause of disability and death, affecting nearly 30 million people worldwide each year, most of which are ischemic strokes [1]. Stroke can not only cause immediate death but also induce various complications such as cardiac dysfunction, which is common and is known as the brain–heart interaction [2]. The main symptoms are myocardial injury and arrhythmias [3–5], often accompanied by increased serum cardiac enzymes such as N-terminal pro-brain natriuretic peptide (NT-proBNP) [6, 7]. Importantly, patients without primary heart disease may also develop cardiac dysfunctions, indicating that stroke is the primary cause [8, 9].

Systemic inflammation is the major causative factor for the sequential complications after stroke, especially for the brain–heart interaction [2], but the underlying molecular pathway has not been clarified. Many stroke patients have diabetes, which is a major risk factor for a poor outcome [10]. It is unclear whether and how diabetes affects the brain–heart interaction. Animal studies have shown that middle cerebral artery occlusion (MCAO) increases

Hong-Bin Lin and Guan-Shan Wei have contributed equally to this work.

Electronic supplementary material The online version of this article (https://doi.org/10.1007/s12264-020-00544-0) contains supplementary material, which is available to authorized users.

✉ Hong-Fei Zhang
zhanghongfei@smu.edu.cn

Shi-Yuan Xu
xsy998@smu.edu.cn

Zhi-Jian You
13928460320@163.com

1 Department of Anesthesiology, Zhujiang Hospital of Southern Medical University, Guangzhou 510220, China

2 Department of Anesthesiology, Shenzhen SAMII Medical Center, Shenzhen 518118, China

3 Department of Anesthesiology, The Second Affiliated Hospital, Shantou University Medical College, Shantou 515041, China

4 University of Ottawa Heart Institute and Department of Cellular and Molecular Medicine, University of Ottawa, Ontario, K1N, Canada

catecholamine levels [11] and impairs cardioprotective signaling pathways [12], thus inducing cardiac dysfunction and cardiomyocyte injury. Other studies have suggested that ischemic stroke induces arrhythmia by impairing calcium and other ionic currents in ventricular cardiomyocytes [13–15]. Pro-inflammatory factors [16] and chronic inflammation [17] might also be involved in the cardiac dysfunction induced after ischemic stroke. An important component of inflammation, the NLR family pyrin domain-containing 3 (NLRP3) inflammasome, has been attested to participate in many inflammatory diseases including type 2 diabetes mellitus, atherosclerosis, cardiovascular diseases, and neurodegenerative diseases [18–22]. Our previous study has shown that inhibition of the NLRP3 inflammasome ameliorates ischemic stroke injury in diabetic mice [23]. However, the role of the NLRP3 inflammasome in the brain–heart interaction and the corresponding mechanisms have not been studied in diabetes.

NLRP3 inflammasomes are mainly activated in macrophages, especially in M1-polarized macrophages [24]. M1-polarized macrophages are classified as showing pro-inflammatory status, while M2-polarized macrophages are alternatively activated macrophages associated with anti-inflammatory activity [25, 26]. We hypothesized that the polarization status of macrophages may play a dominant role in the brain–heart interaction in diabetes. To investigate whether ischemic stroke induce cardiac dysfunction, we used an ischemic stroke mouse model by applying the MCAO procedure. Afterwards, we investigated whether diabetic status aggravates cardiac dysfunction after stroke using a type 2 diabetes mouse model. Furthermore, we studied the role of NLRP3 and the polarized macrophages responsible in the brain–heart interaction. The sequential questions we have addressed provide a causative pathway for the brain–heart interaction, and shed light on therapeutic targets for diabetic patients after ischemic stroke.

Materials and Methods

Animals

This study was approved by the Medical Faculty Ethics Committee of Southern Medical University. Male C57BL/6 J mice (4–6 weeks old, 14–18 g) were purchased from the Animal Experimental Center of Southern Medical University. All experimental animals were maintained under a 12-h light and 12-h dark cycle and were supplied with adequate food and water before experiments.

Type 2 Diabetes Mellitus Mouse Model

This followed the protocol of our previous study [23]. Briefly, to establish a diabetic mouse model, we initially fed each mouse on a high-fat diet (Guangdong Medical Laboratory Animal Center, Guangzhou, China) for 3 weeks, then gave an intraperitoneal injection of 0.1 g/kg streptozotocin (STZ, Sigma, St. Louis, MO, USA). After that, mice were fed with the high-fat diet for another 4 weeks. The blood glucose concentration was measured after fasting for 8 h on days 1, 22, 36, and 50. The criterion for a type 2 diabetes mellitus mouse was a fasting glucose > 10.0 mmol. Non-diabetic mice were housed in the same environment, fed with a normal diet, and given an intraperitoneal injection of vehicle (saline).

Focal Cerebral Ischemia Mouse Model

The ischemic stroke mouse model was generated by MCAO following the protocol of our previous study [23]. In brief, mice were anesthetized with 2% isoflurane (RWD Life Science Co., Ltd, Shenzhen, China). After a midline neck incision, a 4–0 nylon monofilament (Yushun Bio Technology Co. Ltd., Pingdingshan, China) was inserted into the right MCA to block the blood flow. The monofilament was withdrawn after blocking the flow for 60 min. Sham-operated mice underwent the same procedure without inserting the monofilament. A heating pad was used to keep the rectal temperature at 37 ± 0.5 °C during the whole procedure. Cerebral blood flow (CBF) was evaluated using the 2-dimensional laser speckle imaging system and laser Doppler flowmetry (Fig. 1B). Mice were considered to be ischemic stroke models when the blood flow in the ischemic core decreased by $> 70\%$, and were included in further analyses.

Cardiac Function Measurements

Echocardiography was used to evaluate cardiac function before stroke and 4 weeks later. The procedure followed that described by Ay *et al.* [9]. In brief, the thoracic hair was shaved and ultrasound transmission gel applied. Serial cardiac ultrasound analyses used the Vevo 2100 ultrasound imaging system (VisualSonics Inc., Toronto, Canada) with a 30-MHz probe. Ejection fraction (EF) and fractional shortening (FS) were calculated from 2-dimensionally targeted M-mode tracings. All primary measurement data were processed and analyzed using the Vevo 2100 analysis system and repeated three times.

Neurological Scoring

The neurological deficit, based on the motor behavior and level of consciousness of each mouse [23], was scored on days 1, 7, 14, 21, and 28 after MCAO. Scoring was done by a researcher who was blinded to the experimental grouping.

Survival Analysis

The vital signs of each mouse were checked every 24 h after MCAO. Times of death were recorded, and data from survivors were collected for 28 days.

Histological and Immunohistochemical Assessment

The whole brain was removed immediately after euthanasia by isoflurane overdose on day 28 after MCAO. The right hemispheric atrophy volume (right hemispheric volume/left hemispheric volume) after stroke was assessed using ImageJ (version 1.49, National Institutes of Health, Bethesda, MD, USA), then sectioned for staining in 2% 2,3,5-triphenyltetrazolium chloride (TTC). The heart was isolated and weighed after expressing the blood, then fixed in 4% paraformaldehyde before being embedded in paraffin and coronal sections of the ventricle were cut at 6 μm. PicroSirius Red staining was used to assess the interstitial collagen fraction. For immunostaining, the following primary antibodies were used: mouse anti-IBA1 (1:1000, Thermo Fisher, Waltham, MA, USA), rabbit anti-NLRP3 (1:1000, Thermo Fisher, Waltham, MA, USA), mouse anti-caspase-1 (1:250; Santa Cruz Biotechnology, Santa Cruz, CA, USA), and rabbit anti-α-smooth muscle actin (1:1000; Cell Signaling Technology, Danvers, MA, USA). All heart sections for analysis were processed at the same time in a single round of the immunohistochemical experiment.

Real-Time Quantitative RT-PCR

RT-PCR was used to measure mRNA expression (primer sequences are listed in Table 1). RNA was extracted from the apex myocardial tissue using the RNAiso Plus kit (9109, Takara Bio Inc., Shiga, Japan). cDNA was generated using the Veriti PCR System (Applied Biosystems Inc., Beverly, MA, USA). RT-PCR was applied using the SYBR Green kit (RR820A, Takara Bio Inc.) using 10 μL cDNA. The mRNA expression was normalized to the housekeeping gene β-actin.

Western Blot Assay

Apex myocardial tissue from each heart was ground with a Tissue grinder (JXFSTPRP-32, Shanghai Jingxin, Co,. Ltd, China) and total protein was isolated. The primary antibodies were: anti-NLRP3 (1:3000; 15101, Cell Signaling Technology), anti-caspase-1 (1:3000; sc-56036, Santa Cruz Biotechnology), and anti-α-tubulin (1:10000; RM2007, Beijing Ray Antibody Biotech, China).

ELISA for NT-proBNP Analysis

Blood plasma was collected on day 28 after MCAO or sham operation. Samples were analyzed for the concentrations of NT-proBNP using an ELISA kit according to the manufacturer's protocol (E-EL-M0834c, Elabscience Biotechnology Co. Ltd., Wuhan, China).

Statistical Analysis

All data are expressed as the mean ± SD. Differences between groups were compared using Student's t test for single comparisons or one-way variance (ANOVA) for continuous variables with a normal distribution. The means across groups with repeated measurements over time were analyzed using repeated-measures ANOVA. Survival comparisons were analyzed using Prism7 software (GraphPad7, San Diego, CA, USA). Statistical significance was defined as $P < 0.05$.

Results

Ischemic Stroke Induces Cardiac Dysfunction in the MCAO Mouse Model

To study the brain–heart interaction after ischemic stroke, we used the MCAO mouse model [23] and tested cardiac functions before and afterwards. MCAO for 60 min induced ischemic stroke by blocking the major cerebral blood flow (Fig. 1A, B); this was further confirmed by the decreased right hemispheric volume on day 28 after surgery (Fig. 1C). Compared to the sham-operated mice, although there was no difference in the echocardiography before MCAO (Fig. S1A), it showed reduced EF and FS on day 28 in the MCAO mice (Fig. 1D), demonstrating impaired cardiac function after ischemic stroke. We also found that the plasma level of NT-proBNP (a major biomarker of cardiac dysfunction) was significantly elevated in MCAO (Fig. 1G). When checking the morphological changes in the heart, enlargement was revealed by the heart/body weight ratio (Fig. 1H). Furthermore, a higher cardiac interstitial collagen fraction was seen in ventricular sections from MCAO mice than in those from the sham group (Fig. 1E). Consistent with the morphological changes, the fibrotic protein α-SMA was also higher in the ventricles from stroke mice than in sham mice

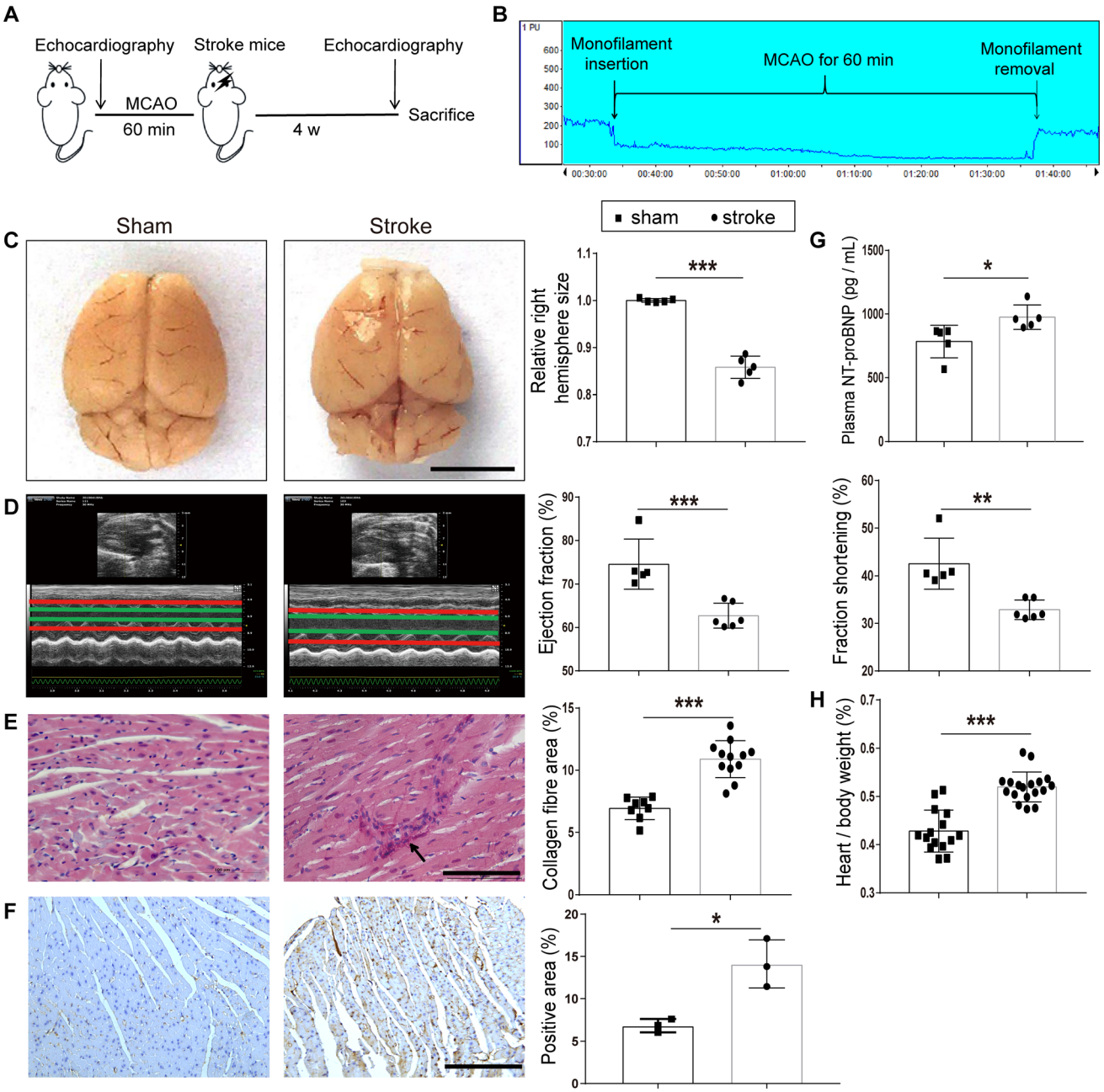

Fig. 1 Cardiac dysfunction in MCAO mice. **A** Diagram of the MCAO model echocardiography protocol. **B** Example of laser Doppler measurement showing that MCAO sharply reduces cerebral blood flow (CBF) when the monofilament is inserted. CBF is restored after the monofilament is removed. **C** Changes in brain morphology and right hemispheric atrophy in the sham and stroke groups (n = 5 per group). **D** Left, examples of echocardiography in mice at day 28 after MCAO. Right, bar graphs show the ejection fraction and fractional shortening in the sham (n = 5) and stroke groups (n = 6). **E** Left, PicroSirius Red staining for interstitial collagen (arrow) in cardiac ventricular tissue. Right, interstitial collagen fraction in sham (n = 8) and stroke groups (n = 12). **F** Left, immunohistochemical staining for α-SMA in cardiac ventricular tissue. Right, α-SMA-positive area in the sham and stroke groups (n = 3 per group). **G** Plasma levels of NT-proBNP in the sham and stroke groups (n = 5 per group). **H** Heart/body weight ratio in the sham (n = 15) and stroke groups (n = 18). Data are expressed as the mean ± SD. $^{*}P < 0.05$; $^{**}P < 0.01$; $^{***}P < 0.001$ (Student's t-test). Magnification, 400 × in **E** and 200 × in **F**; scale bars, 5 mm in **C**, 100 μm in **E**, and 50 μm in **F**.

Table 1 Primer list.

Gene	Forward primer: 5′-3′	Reverse primer: 5′-3′
NLRP3	ATTACCCGCCCGAGAAAGG	TCGCAGCAAAGATCCACACAG
Caspase-1	AATACAACCACTCGTACACGTC	AGCTCCAACCCTCGGAGAAA
IL-1β	GAAATGCCACCTTTTGACAGTG	TGGATGCTCTCATCAGGACAG
β-actin	GTGCTATGTTGCTCTAGACTTCG	ATGCCACAGGATTCCATACC
M1 markers		
CD16	TTTGGACACCCAGATGTTTCAG	GTCTTCCTTGAGCACCTGGATC
INOS	CAAGCACCTTGGAAGAGGAG	AAGGCCAAACACAGCATACC
TNF-α	CGTCGTAGCAAACCACCAAG	GAGATAGCAAATCGGCTGACG
M2 markers		
Ym1/2	CAGGGTAATGAGTGGGTTGG	CACGGCACCTCCTAAATTGT
IL-10	TGGACAACATACTGCTAACCGAC	CCACTGCCTTGCTCTTATTTTC
TGF-β	TGCGCTTGCAGAGATTAAAA	CGTCAAAAGACAGCCACTCA

NLRP3, NLR pyrin domain containing 3; IL, interleukin; INOS, inducible nitric oxide synthase; TNF-α, tumor necrosis factor alpha; TGF-β, transforming growth factor beta.

(Fig. 1F). These results demonstrated a brain–heart interaction in the MCAO mouse model.

Cardiac Dysfunction is More Severe in Diabetic Stroke

To address whether diabetic status affects cardiac dysfunction after ischemic stroke, we established a type 2 diabetes mouse model by a high-fat diet and intraperitoneal STZ injection, which showed a sustained high glucose level until day 50 (Fig. 2B). The MCAO procedure was done 4 weeks after STZ injection and cardiac functions were measured accordingly (Fig. 2A). Comparable infarcted regions and right hemisphere size were induced after MCAO in both diabetic and non-diabetic mice (Fig. 2C). Surprisingly, although there was no difference in the echocardiography before MCAO (Fig. S1B), diabetic mice exhibited a robust reduction of EF and FS by day 28 post-stroke (Fig. 2D), indicating a susceptibility to post-stroke cardiac dysfunction in diabetes. Furthermore, a higher level of plasma NT-proBNP (Fig. 2D) and heart/body weight ratio (Fig. 2H) were detected in diabetic stroke mice compared to the non-diabetic stroke mice. Correlated with the echocardiography and NT-proBNP changes, the cardiac interstitial collagen fraction and fibrotic protein α-SMA also increased significantly in the diabetic stoke myocardium compared to the non-diabetic stroke mice (Fig. 2E–F). Our data indicated that diabetic status worsens cardiac dysfunction, the cardiac interstitial collagen fraction, and hypertrophy in mice with ischemic stroke.

Diabetic Status Worsens the Overall Outcome of Stroke

As cardiac dysfunction was more severe in diabetic stroke mice, we set out to determine how diabetes affects the neurological deficits and the overall outcome in our MCAO model. Consistent with other reports [27], our diabetic stroke mice showed higher neurological deficit scores at days 1, 7, and 28 after MCAO (Fig. 3A). Referring to the overall mortality rate, fewer diabetic stroke mice survived at the end of day 28 compared to the non-diabetic group (Fig. 3B). These data suggested that not only the cardiac dysfunction but also the overall outcome was affected by diabetic status in the MCAO mouse model.

NLRP3 Activation is Indispensable for Brain–Heart Interaction in Diabetic Stroke

The results of cardiac dysfunction and worse neurologic outcomes indicated that a stronger brain–heart interaction exists in diabetic stroke mice. Taking into account that both stroke and diabetes exhibit NLRP3 activation and worsen the respective outcomes, we tested the corresponding mRNA and protein levels. As anticipated, the NLRP3 mRNA and protein levels, as well as caspase-1 and IL-1β levels showed more robust elevation in the myocardium from diabetic stroke mice than those from non-diabetic mice (Fig. 4A–C). Surprisingly, the NLRP3 inhibitor CY-09 (HY-103666; MedChem Express, Monmouth Junction, NJ, USA) sufficiently restored the cardiac function, showing improved EF and FS compared with the vehicle group (Fig. 4D). Morphological studies also revealed a reduction in the heart/body weight ratio (Fig. 4G), the cardiac interstitial collagen fraction (Fig. 4E), and fibrotic protein α-SMA expression after CY-09 administration

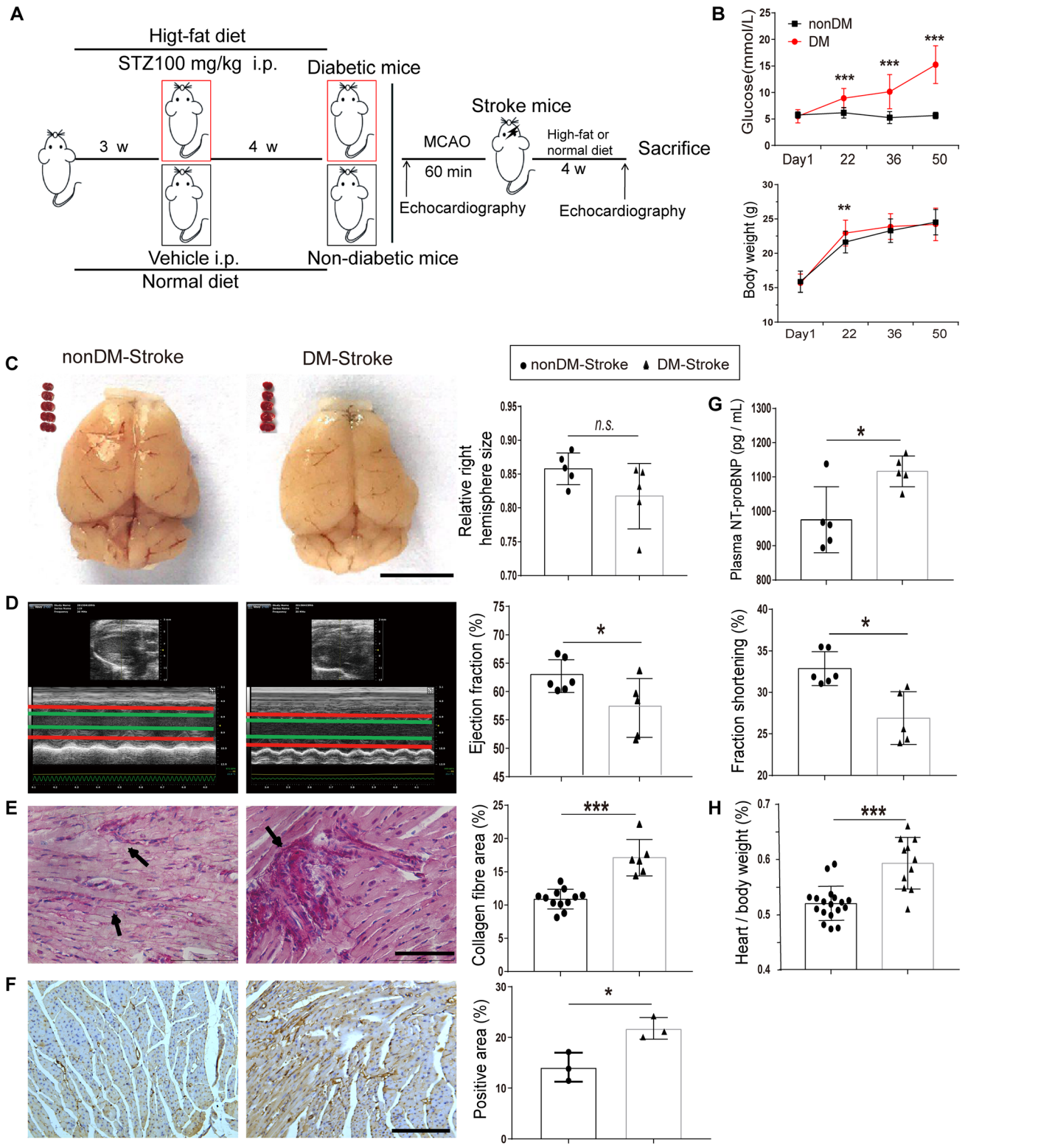
A
Higt-fat diet
STZ100 mg/kg i.p.
Diabetic mice
3 w
4 w
Stroke mice
MCAO
60 min
High-fat or normal diet
4 w
Sacrifice
Echocardiography
Echocardiography
Vehicle i.p.
Non-diabetic mice
Normal diet
B
nonDM
DM
Glucose(mmol/L)
Day1 22 36 50
Body weight (g)
C
nonDM-Stroke
DM-Stroke
nonDM-Stroke DM-Stroke
Relative right hemisphere size
n.s.
G
Plasma NT-proBNP (pg / mL)
D
Ejection fraction (%)
Fraction shortening (%)
E
Collagen fibre area (%)
H
Heart / body weight (%)
F
Positive area (%)

◀**Fig. 2** Ischemic stroke induces severe cardiac dysfunction in diabetic mice. **A** Diagram of protocols for establishing the type 2 diabetes mellitus and MCAO mouse models. **B** Time courses of blood glucose and body weight showing significant increases from day 22 in diabetic mice (n = 22) compared with non-diabetic mice (n = 33). **C** Brain morphology and TTC staining in coronal brain sections from non-diabetic stroke (nonDM-Stroke) and diabetic stroke (DM-Stroke) mice (n = 5 per group). **D** Echocardiographic traces (left) and ejection fraction and fractional shortening (right) in nonDM-Stroke (n = 6) and DM-Stroke (n = 5) mice. **E** Left, PicroSirius red staining for interstitial collagen (arrows) in cardiac ventricular tissue. Right, interstitial collagen fraction in nonDM-Stroke (n = 12) and DM-Stroke (n = 6) mice. **F** Left, immunohistochemical staining for α-SMA in cardiac ventricular tissue. Right, α-SMA-positive area in nonDM-Stroke and DM-Stroke (n = 3 per group) mice. **G** Plasma levels of NT-proBNP in nonDM-Stroke and DM-Stroke (n = 5 per group) mice. **H** Heart/body weight in nonDM-Stroke (n = 18) and DM-Stroke (n = 11) mice. DM, diabetes mellitus; STZ, streptozotocin; i.p. intraperitoneal. Data are expressed as the mean ± SD. $*P < 0.05$; $**P < 0.01$; $***P < 0.001$, *n.s.* not significant (Student's t-test). Magnification, 400 × in **E** and 200 × in **F**; scale bars, 5 mm in **C**, 100 μm in **E**, and 50 μm in **F**.

(Fig. 4F). The inhibitory effect of CY-09 on NLRP3 activation was further confirmed in myocardial tissue as reduced expression of NLRP3, caspase-1, and IL-1β compared to the vehicle group (Fig. 4H–I). These results identified a role of NLRP3 in the brain–heart interaction in the diabetic mouse.

M1 Macrophages are Responsible for NLRP3-Mediated Brain–Heart Interaction

NLRP3 inflammasomes are mainly from M1- rather than M2-polarized macrophages [24]. To dissect the source of the NLRP3 inflammasomes, we confirmed the expression of the macrophage marker IBA1 in the myocardium from diabetic stroke mice (Fig. 5A). Furthermore, polarized markers were measured and indicated that M1- (revealed by CD16, iNOS, and TNF-α), but not M2- (revealed by Ym1/2, IL-10, and TGF-β) polarized macrophages were the dominant type infiltrating the myocardium in post-diabetic stroke (Fig. 5B). The expression levels of these markers implied that M1-polarized macrophage–NLRP3 inflammasome activation is an indispensable molecular pathway. Considering the restorative effects of the NLRP3 inhibitor CY-09 on the brain–heart interaction, we tested whether it affects the macrophage polarization status. Surprisingly, CY-09 significantly elevated the mRNA expression levels of Ym1/2, IL-10, and TGF-β, while decreasing the levels of CD16, iNOS, and TNF-α in diabetic stroke mice compared to the vehicle group (Fig. 5C). The results indicated that the infiltrating macrophages switched to M2 after CY-09 administration,

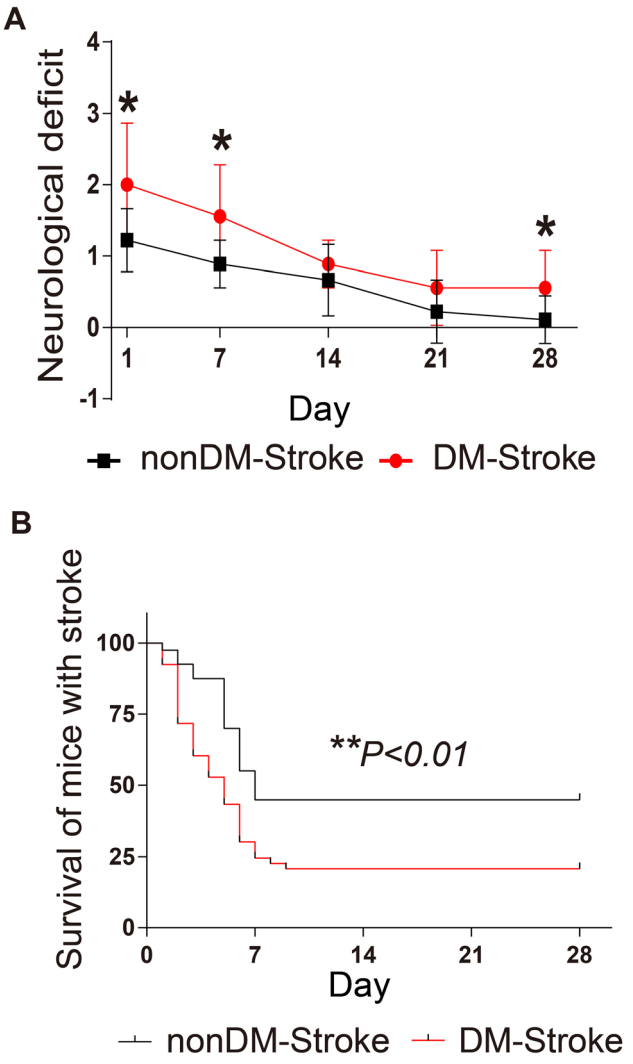

Fig. 3 Diabetes leads to a worse prognosis after ischemic stroke. **A** Neurological deficit scores in nonDM-Stroke and DM-Stroke mice at 24 h and 7, 14, 21, and 28 days (n = 9 per group). **B** Mortality until day 28 in nonDM-Stroke (n = 40) and DM-Stroke (n = 53) mice. nonDM-Stroke, non-diabetic stroke group; DM-Stroke, diabetic stroke group. Data are expressed as the mean ± SD. $*P < 0.05$; $**P < 0.01$ (Student's t-test in **A** and log-rank test in **B**).

strongly supporting the specific role of NLRP3 in the brain–heart interaction.

The overall results demonstrated that the brain–heart interaction is due to the infiltration of M1-polarized macrophages into the myocardium after diabetic stroke. This infiltration sequentially induces NLRP3 inflammasome activation and impairs cardiac function, which is responsible for the poor outcome in diabetic stroke (Fig. 6).

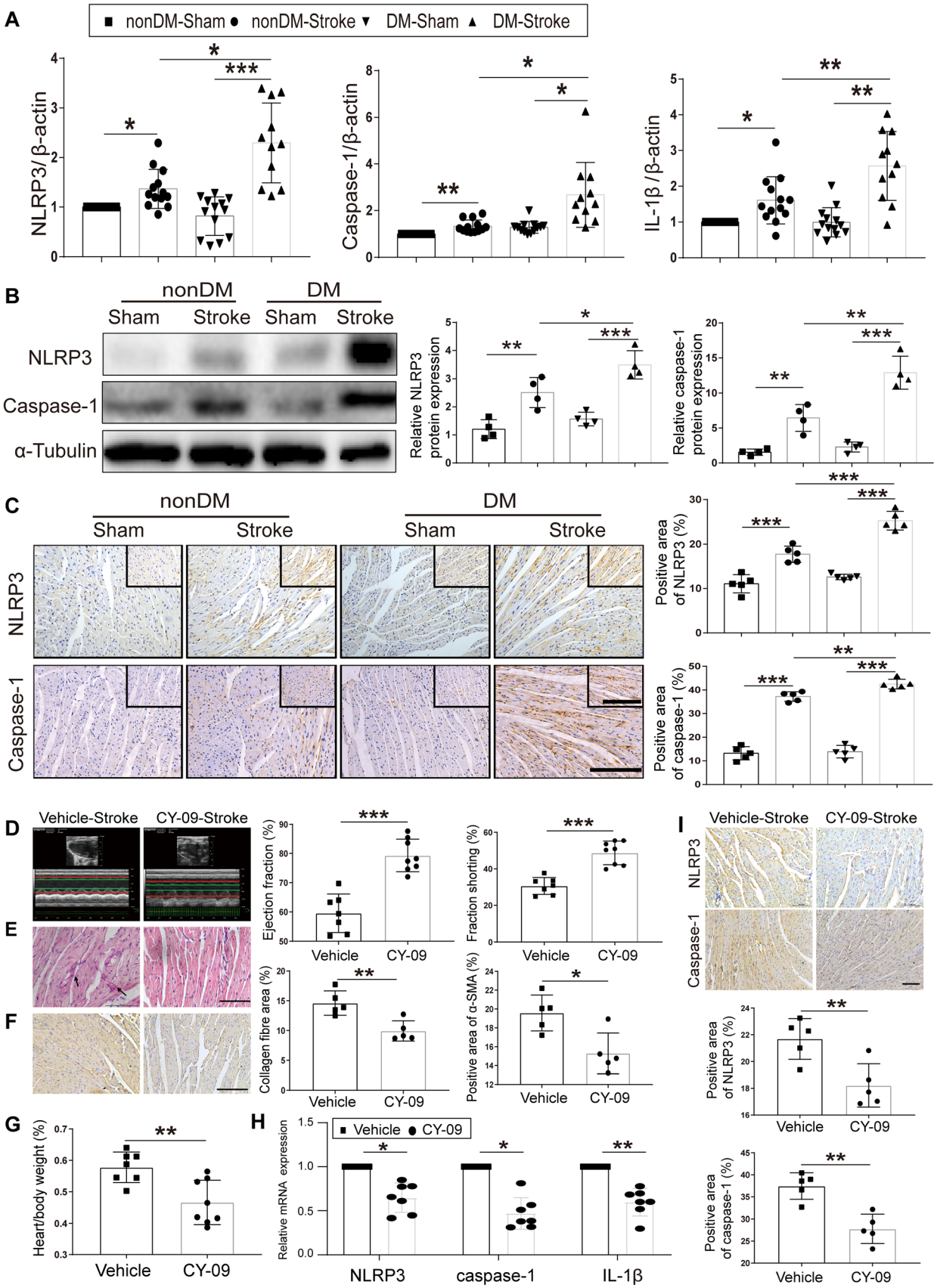
A
nonDM-Sham
nonDM-Stroke
DM-Sham
DM-Stroke
NLRP3/β-actin
Caspase-1/β-actin
IL-1β /β-actin
B
nonDM
DM
Sham
Stroke
Sham
Stroke
NLRP3
Caspase-1
α-Tubulin
Relative NLRP3 protein expression
Relative caspase-1 protein expression
C
nonDM
DM
Sham
Stroke
Sham
Stroke
NLRP3
Caspase-1
Positive area of NLRP3 (%)
Positive area of caspase-1 (%)
D
Vehicle-Stroke
CY-09-Stroke
Ejection fraction (%)
Fraction shorting (%)
Vehicle
CY-09
E
F
Collagen fibre area (%)
Positive area of α-SMA (%)
G
Heart/body weight (%)
H
Vehicle
CY-09
Relative mRNA expression
NLRP3
caspase-1
IL-1β
I
Vehicle-Stroke
CY-09-Stroke
NLRP3
Caspase-1
Positive area of NLRP3 (%)
Positive area of caspase-1 (%)

◀**Fig. 4** NLRP3 activation plays an important role in the brain–heart interaction in diabetic stroke. **A** Relative gene expression of NLRP3, caspase-1, and IL-1β in apex myocardial tissue. β-Actin served as an endogenous reference gene (n = 13 in nonDM-Sham, nonDM-stroke, and DM-Sham; n = 11 in DM-Stroke). **B** Left, NLRP3 and caspase-1 in apex myocardial tissue indicated by western blot. Right, integrated density value of relative protein expression of NLRP3 and caspase-1 (n = 4 per group). **C** Left, protein expression of NLRP3 and caspase-1 in cardiac ventricular tissue by immunocytochemistry. Right, NLRP3, caspase-1-positive area in different group mice (n = 5 per group). **D** Echocardiographic measurement of ejection fraction and fractional shortening in Vehicle-Stroke (n = 7) and CY-09-Stroke (n = 8) mice. **E** Left, PicroSirius red staining for interstitial collagen (arrows) in ventricular tissue. Middle, interstitial collagen fraction in Vehicle-Stroke and CY-09-Stroke mice (n = 5 per group). **F** α-SMA immunohistochemical staining (left) of ventricular tissue and α-SMA area (right) in Vehicle-Stroke and CY-09-Stroke mice (n = 5 per group). **G** Heart/body weight in Vehicle-Stroke (n = 7) and CY-09-Stroke (n = 8) mice. **H** Relative gene expression of NLRP3, caspase-1, and IL-1β in apex myocardial tissue (n = 7 per group). **I** Top, immunohistochemical staining for NLRP3 and caspase-1 in cardiac ventricular tissue. Bottom, NLRP3 and caspase-1-positive area in Vehicle-Stroke and CY-09-Stroke mice (n = 5 per group). nonDM-Sham, non-diabetic sham group; nonDM-Stroke, non-diabetic stroke group; DM-Sham, diabetic sham group; DM-Stroke, diabetic stroke group; Vehicle, Vehicle-Stroke group; CY-09, CY-09-Stroke group. Data are expressed as the mean ± SD. $*P < 0.05$; $**P < 0.01$; $***P < 0.001$ (Student's t-test or one-way ANOVA). Magnification, 400 × in **C** (upper right) and **E**; 200 × in **C**, **F**, and **I**; scale bars, 100 μm in **E**; 50 μm in **C**, **F**, and **I**.

Discussion

Our results revealed that severe cardiac dysfunction occurs in diabetic ischemic stroke, shown as the brain–heart interaction, due to NLRP3 inflammasome activation in M1-polarized macrophages. We first provided evidence that diabetic status worsened the cardiac dysfunction, as well as increasing the interstitial collagen fraction and cardiac hypertrophy after stroke in a type 2 diabetes MCAO mouse model. Second, M1-polarized macrophage infiltration and NLRP3 inflammasome activation were enhanced in the post-stroke myocardium, and were more severe in diabetic mice. Moreover, inhibiting the NLRP3 inflammasome with CY-09 restored the cardiac function and reversed the myocardial morphological changes after ischemic stroke.

Clinical evidence has implied that the brain–heart interaction occurs in the post-stroke stage. Nearly 19% of patients suffer at least one major detrimental cardiac complication within the first 3 months following an acute ischemic stroke [28]. The cardiac dysfunctions include, but are not limited to, impaired pumping action, fibrosis, and hypertrophy. It has been reported that > 50% of stroke patients have left ventricular diastolic dysfunction and 13%–29% have systolic dysfunction [29, 30]. Furthermore, 75%–92% of stroke patients present a new ECG abnormality [31]. By measuring the cardiac function using

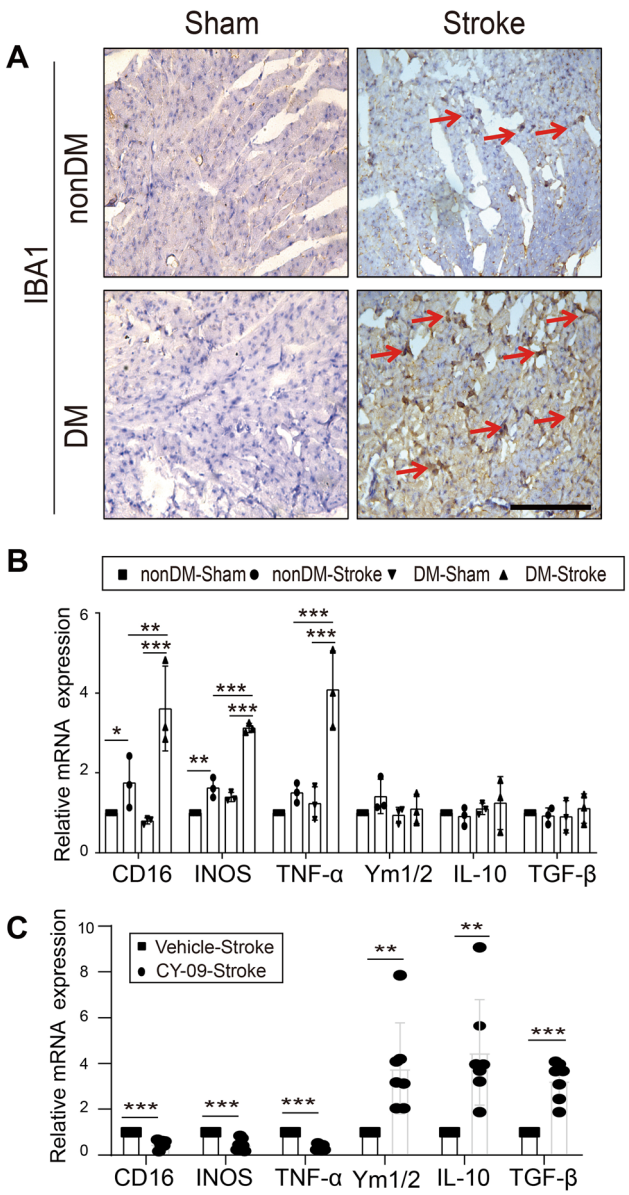

Fig. 5 Macrophages increase and polarize in the brain–heart interaction. **A** Representative immunocytochemical staining for the macrophage marker IBA1 (arrows) in cardiac tissue (magnification, 400 × ; scale bar, 100 μm). **B**, **C** Relative mRNA expression of macrophage-polarization markers in apex myocardial tissue (M1 markers: CD16, INOS, and TNF-α; M2 markers: Ym1/2, IL-10, and TGF-β) (n = 3 in nonDM-Sham, non-DM stroke, DM-Sham and DM-Stroke; n = 7 in Vehicle-Stroke and CY-09-Stroke). IL, interleukin; INOS, inducible nitric oxide synthase; TNF-α, tumor necrosis factor alpha; TGF-β, transforming growth factor beta. Data are expressed as the mean ± SD. $*P < 0.05$; $**P < 0.01$; $***P < 0.001$ (Student's t-test or one-way ANOVA).

echocardiography, we also found remarkable changes after the MCAO procedure in diabetic and non-diabetic mice, indicating the clinical relevance of our methodology.

Many studies have suggested various mechanisms of the brain–heart interaction induced by ischemic stroke,

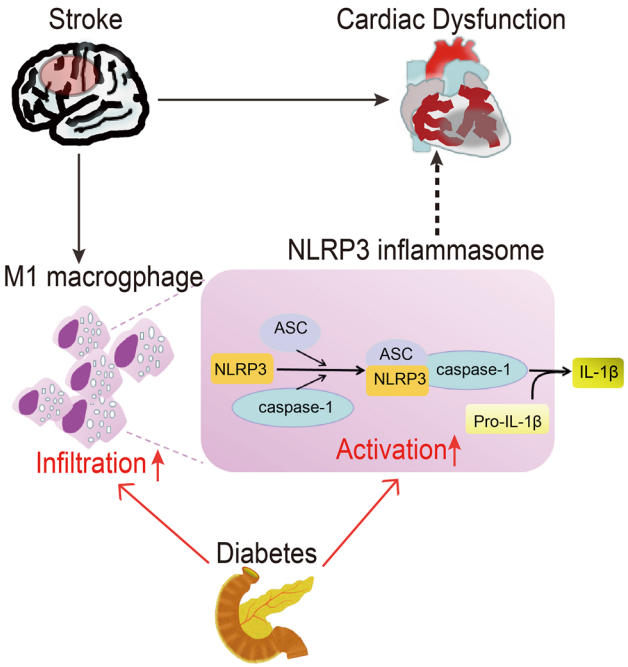

Fig. 6 Schematic of the underlying mechanism for ischemic stroke-induced cardiac dysfunction in the diabetic mouse. M1-polarized macrophage infiltration and NLRP3 inflammasome activation in the heart after ischemic stroke induce cardiac dysfunction. Diabetes mellitus exacerbates the cardiac dysfunction after ischemic stroke through increased M1-polarized macrophage infiltration and NLRP3 inflammasome activation in the heart. NLRP3, NLR pyrin domain containing 3; ASC, apoptosis-associated speck-like protein containing a CARD.

including cardiac autonomic dysfunction after ischemic injury of the insular cortex [32], systemic inflammation, the hypothalamic–pituitary–adrenal axis, blood–brain barrier disruption, and gut microbiome dysbiosis [2, 11]. However, the underlying molecular mechanisms are still far from precisely dissected, especially in diabetic patients. Diabetic status not only exacerbates ischemic brain injury, but also increases post-stroke complications [33, 34]. A clinical study reported that diabetes is an independent predictor of unfavorable outcomes, and mortality increases while the cardiac pumping function decreases after stroke [35]. Another study showed that pioglitazone, a classic hypoglycemic drug, improves the cardiovascular functions of patients after ischemic stroke or transient ischemic attack [36]. These studies point to a role of inflammation in the brain–heart interaction. Chronic inflammation plays an important role in cardiac fibrosis [37] as well as ischemic stroke [38, 39]. Microglial infiltration induced by ischemic stroke increases inflammation by releasing pro-inflammatory cytokines and chemokines such as TNF-α, IL-1β, and vascular cell adhesion protein 1 [40, 41]. As a result, brain tissue releases glial fibrillar acidic protein, S100 and myelin basic protein and sheds extracellular microvesicles, then activates the peripheral immune system [34]. The extracellular microvesicles and pro-inflammatory molecules can recruit macrophages and switch them to M1 polarization [42] and hence activate NLRP3 inflammasomes [43]. Notably, M1-polarized macrophages are closely associated with fibrosis [25]. In our study, the process of M1-polarized macrophage–NLRP3 inflammasome activation was shown to be the molecular pathway for inducing cardiac dysfunction and myocardial fibrosis. CY-09, a specific inhibitor of NLRP3, binds to the ATP-binding motif of the NLRP3 NACHT domain and inhibits NLRP3 ATPase activity, hence inhibiting NLRP3 inflammasome assembly and activation in macrophages [44]. As shown in our study, the anti-inflammatory effect of CY-09 also benefits cardiac functions after diabetic ischemic stroke, providing strong evidence for its clinical relevance.

In summary, our study suggested that diabetic status decreases cardiac function after ischemic stroke by increasing infiltration by M1-polarized macrophages and NLRP3 inflammasome activation. A compensatory mechanism would partially rescue the neurological deficit after stroke [45]. This explains why the neurological deficit gradually recovered although the cardiac morphological changes lasted for at least 28 days. Further study should focus on how to manipulate M1-polarized macrophages to reverse the pathological myocardial changes before they form scar-like tissue after stroke.

Acknowledgements This work was supported by grants from the National Natural Science Foundation of China (81771232 and 81974192) and the Natural Science Foundation of Guangdong Province, China (2019A1515010654).

Conflict of interest The authors claim that there are no conflicts of interest.

References

1. Wang W, Jiang B, Sun H, Ru X, Sun D, Wang L, *et al.* Prevalence, incidence, and mortality of stroke in China: results from a nationwide population-based survey of 480 687 adults. Circulation 2017, 135:759–771.
2. Chen Z, Venkat P, Seyfried D, Chopp M, Yan T, Chen J. Brain–heart interaction: cardiac complications after stroke. Circ Res 2017, 121: 451–468.
3. Yoshimura S, Toyoda K, Ohara T, Nagasawa H, Ohtani N, Kuwashiro T, *et al.* Takotsubo cardiomyopathy in acute ischemic stroke. Ann Neurol 2008, 64: 547–554.
4. Samuels MA. The brain-heart connection. Circulation 2007, 116: 77–84.
5. Kumar S, Selim MH, Caplan LR. Medical complications after stroke. Lancet Neurol 2010, 9: 105–118.
6. Bugnicourt JM, Rogez V, Guillaumont MP, Rogez JC, Canaple S, Godefroy O. Troponin levels help predict new-onset atrial fibrillation in ischaemic stroke patients: a retrospective study. Eur Neurol 2010, 63: 24–28.

7. Cushman M, Judd SE, Howard VJ, Kissela B, Gutierrez OM, Jenny NS, *et al.* N-terminal pro-B-type natriuretic peptide and stroke risk: the reasons for geographic and racial differences in stroke cohort. Stroke 2014, 45: 1646–1650.
8. Cheshire WJ, Saper CB. The insular cortex and cardiac response to stroke. Neurology 2006, 66: 1296–1297.
9. Ay H, Koroshetz WJ, Benner T, Vangel MG, Melinosky C, Arsava EM, *et al.* Neuroanatomic correlates of stroke-related myocardial injury. Neurology 2006, 66: 1325–1329.
10. Ergul A, Abdelsaid M, Fouda AY, Fagan SC. Cerebral neovascularization in diabetes: implications for stroke recovery and beyond. J Cereb Blood Flow Metab 2014, 34: 553–563.
11. Bieber M, Werner RA, Tanai E, Hofmann U, Higuchi T, Schuh K, *et al.* Stroke-induced chronic systolic dysfunction driven by sympathetic overactivity. Ann Neurol 2017, 82: 729–743.
12. Meloux A, Rochette ERL, Cottin Y, Bejot Y, Vergely C. Ischemic stroke increases heart vulnerability to ischemia-reperfusion and alters myocardial cardioprotective pathways. Stroke 2018, 49: 2752–2760.
13. Wang L, Sun L, Zhang Y, Wu H, Li C, Pan Z, *et al.* Ionic mechanisms underlying action potential prolongation by focal cerebral ischemia in rat ventricular myocytes. Cell Physiol Biochem 2009, 23: 305–316.
14. Sun L, Ai J, Wang N, Zhang R, Li J, Zhang T, *et al.* Cerebral ischemia elicits aberration in myocardium contractile function and intracellular calcium handling. Cell Physiol Biochem 2010, 26: 421–430.
15. Sun L, Du J, Zhang G, Zhang Y, Pan G, Wang L, *et al.* Aberration of L-type calcium channel in cardiac myocytes is one of the mechanisms of arrhythmia induced by cerebral ischemia. Cell Physiol Biochem 2008, 22: 147–156.
16. Ishikawa H, Tajiri N, Vasconcellos J, Kaneko Y, Mimura O, Dezawa M, *et al.* Ischemic stroke brain sends indirect cell death signals to the heart. Stroke 2013, 44: 3175.
17. Acosta SA, Mashkouri S, Nwokoye D, Lee JY, Borlongan CV, Ishikawa H, *et al.* Chronic inflammation and apoptosis propagate in ischemic cerebellum and heart of non-human primates. Oncotarget 2017, 8: 102820–102834.
18. Vandanmagsar B, Youm YH, Ravussin A, Galgani JE, Stadler K, Mynatt RL, *et al.* The NLRP3 inflammasome instigates obesity-induced inflammation and insulin resistance. Nat Med 2011, 17: 179–188.
19. Liu D, Zeng X, Li X, Mehta JL, Wang X. Role of NLRP3 inflammasome in the pathogenesis of cardiovascular diseases. Basic Res Cardiol 2017, 113: 5.
20. Zeng J, Chen Y, Ding R, Feng L, Fu Z, Yang S, *et al.* Isoliquiritigenin alleviates early brain injury after experimental intracerebral hemorrhage via suppressing ROS- and/or NF-kappaB-mediated NLRP3 inflammasome activation by promoting Nrf2 antioxidant pathway. J Neuroinflammation 2017, 14: 119.
21. Peng Y, Liu B, Pei S, Zheng D, Wang Z, Ji T, *et al.* Higher CSF levels of NLRP3 inflammasome is associated with poor prognosis of anti-N-methyl-D-aspartate receptor encephalitis. Front Immunol 2019, 10: 905.
22. Xu L, Qiu X, Wang S, Wang Q, Zhao XL. NMDA receptor antagonist MK801 protects against 1-bromopropane-induced cognitive dysfunction. Neurosci Bull 2019, 35: 347–361.
23. Hong P, Li FX, Gu RN, Fang YY, Lai LY, Wang YW, *et al.* Inhibition of NLRP3 inflammasome ameliorates cerebral ischemia-reperfusion injury in diabetic mice. Neural Plast 2018, 2018: 1–8.
24. Liu W, Zhang X, Zhao M, Zhang X, Chi J, Liu Y, *et al.* Activation in M1 but not M2 macrophages contributes to cardiac remodeling after myocardial infarction in rats: a critical role of the calcium sensing receptor/NRLP3 inflammasome. Cell Physiol Biochem 2015, 35: 2483–2500.
25. Ploeger DT, Hosper NA, Schipper M, Koerts JA, de Rond S, Bank RA. Cell plasticity in wound healing: paracrine factors of M1/M2 polarized macrophages influence the phenotypical state of dermal fibroblasts. Cell Commun Signal. 2013, 11: 29.
26. Kanazawa M, Ninomiya I, Hatakeyama M, Takahashi T, Shimohata T. Microglia and monocytes/macrophages polarization reveal novel therapeutic mechanism against stroke. Int J Mol Sci 2017, 18: 2135.
27. Ma S, Wang J, Wang Y, Dai X, Xu F, Gao X, *et al.* Diabetes mellitus impairs white matter repair and long-term functional deficits after cerebral ischemia. Stroke 2018, 49: 2453–2463.
28. Marto JP, Kauppila LA, Jorge C, Calado S, Viana-Baptista M, Pinho-E-Melo T, *et al.* Intravenous thrombolysis for acute ischemic stroke after recent myocardial infarction: case series and systematic review. Stroke 2019, 50: 2813–2818.
29. Park HK, Kim BJ, Yoon CH, Yang MH, Han MK, Bae HJ. Left ventricular diastolic dysfunction in ischemic stroke: functional and vascular outcomes. J Stroke 2016, 18: 195–202.
30. Prosser J, MacGregor L, Lees KR, Diener HC, Hacke W, Davis S. Predictors of early cardiac morbidity and mortality after ischemic stroke. Stroke 2007, 38: 2295–2302.
31. Khechinashvili G, Asplund K. Electrocardiographic changes in patients with acute stroke: a systematic review. Cerebrovasc Dis 2002, 14: 67–76.
32. Krause T, Werner K, Fiebach JB, Villringer K, Piper SK, Haeusler KG, *et al.* Stroke in right dorsal anterior insular cortex Is related to myocardial injury. Ann Neurol 2017, 81: 502–511.
33. Jia Q, Zhao X, Wang C, Wang Y, Yan Y, Li H, *et al.* Diabetes and poor outcomes within 6 months after acute ischemic stroke: the China national stroke registry. Stroke 2011, 42: 2758–2762.
34. Scheitz JF, Nolte CH, Doehner W, Hachinski V, Endres M. Stroke heart syndrome: clinical presentation and underlying mechanisms. Lancet Neurol 2018, 17: 1109–1120.
35. Siedler G, Sommer K, Macha K, Marsch A, Breuer L, Stoll S, *et al.* Heart failure in ischemic stroke: relevance for acute care and outcome. Stroke 2019, 50: 3051–3056.
36. Young LH, Viscoli CM, Schwartz GG, Inzucchi SE, Curtis JP, Gorman MJ, *et al.* Heart failure after ischemic stroke or transient ischemic attack in insulin-resistant patients without diabetes mellitus treated with pioglitazone. Circulation 2018, 138: 1210–1220.
37. Zhao Q, Yan T, Li L, Chopp M, Venkat P, Qian Y, *et al.* Immune response mediates cardiac dysfunction after traumatic brain injury. J Neurotrauma 2018, 36: 619–629.
38. Chen J, Cui C, Yang X, Xu J, Venkat P, Zacharek A, *et al.* MiR-126 affects brain-heart interaction after cerebral ischemic stroke. Transl Stroke Res 2017, 8: 374–385.
39. Doll DN, Barr TL, Simpkins JW. Cytokines: their role in stroke and potential use as biomarkers and therapeutic targets. Aging Dis 2014, 5: 294–306.
40. Iadecola C, Anrather J. The immunology of stroke: from mechanisms to translation. Nat Med 2011, 17: 796–808.
41. Yilmaz G, Granger DN. Leukocyte recruitment and ischemic brain injury. Neuromolecular Med 2010, 12: 193–204.
42. Singla DK, Johnson TA, Tavakoli Dargani Z. Exosome treatment enhances anti-inflammatory M2 macrophages and reduces inflammation-induced pyroptosis in doxorubicin-induced cardiomyopathy. Cells 2019, 8:1224.
43. Tschopp J, Schroder K. NLRP3 inflammasome activation: the convergence of multiple signalling pathways on ROS production? Nat Rev Immunol 2010, 10: 210–215.
44. Jiang H, He H, Chen Y, Huang W, Cheng J, Ye J, *et al.* Identification of a selective and direct NLRP3 inhibitor to treat inflammatory disorders. J Exp Med 2017, 214: 3219–3238.
45. Cassidy JM, Cramer SC. Spontaneous and therapeutic-induced mechanisms of functional recovery after stroke. Transl Stroke Res 2017, 8: 33–46.